# Bachelor of Science in Medicine Degree Program
# End of Term Final Report

Office of Graduate and
Advanced Degrees
Education in Medicine Max
Rady College
of Medicine
Rady Faculty of
Health Sciences
University of Manitoba

**Student Name:** Evan Kerr **Date:** August 3, 2022

**Project Title:** Enhanced Cutaneous Wound Closure via Adipose-Derived Stem Cell Paracrine Signaling

**Primary Supervisor Name:** Dr Afshin Raouf
**Department:** Immunology

**Co-Supervisor Name:** Dr Edward Buchel
**Department:** Surgery

**Summary (250 words max single spaced):**
Chronic non-healing cutaneous wounds drastically reduce the quality of life for afflicted patients and costs healthcare systems over $50 billion annually. Clinical management of these wounds remains a challenge as current treatments are of limited efficacy. Recently, research in stem cell therapies for wound healing has started to gain more momentum. The aim of this study was to demonstrate that the stromal vascular fraction (SVF), which contains adipose-derived stem cells (ADSC), could accelerate keratinocyte wound closure without direct cell-cell contact and to identify potential cytokines, chemokines and growth factors involved. In-vitro wound closure assays were set up using primary human epidermal keratinocytes, primary (P0) SVF obtained from patients' fat grafts and their matching passaged (P3) SVF. SVF cells were plated on porous membranes of transwell inserts that prevent cell migration while allowing free diffusion of secreted proteins. Keratinocytes were placed in the bottom chamber with a scratch to simulate wound area. Scratch areas were monitored for 36h and following wound closure, media from each well was harvested and analyzed using a panel of 71 different cytokines, chemokines, and growth factors. Our results show that wound closure was accelerated 1.5-fold with P0-SVF and nearly 2-fold with P3-SVF compared to controls. Additionally, six cytokines were significantly upregulated in SVF-keratinocyte cultures during wound closure, namely; IL-6, IL-8, ENA-78, G-CSF, GRO- , and MCP-1. Identification of secreted factors responsible for the acceleration of wound healing is the first step toward designing a standardized cell-free therapy to treat millions of patients with chronic non-healing wounds annually.

Student Signature [redacted]

Primary Supervisor Signature
Afshin Raouf
Digitally signed by Afshin Raouf
Date: 2022.08.04 14:15:33 -05'00'

**Acknowledgments**: I gratefully acknowledge the sole or partial funding support from the following sponsors;

H.T. Thorlakson Foundation
Dean, College of Medicine
Research Manitoba

Manitoba Medical Service Foundation (MMSF)
Vice-Dean, Research Rady FHS
Health Sciences Centre Research Foundation
Heart and Stroke Foundation

Sponsorship if different than above;

## Introduction

Chronic non-healing cutaneous wounds are defined as wounds that fail to close for four weeks or longer, and common etiologies present as diabetic foot ulcers, burns, pressure ulcers, and venous ulcers (Powers *et al*. 2019). These wounds continue to burden the healthcare system financially and significantly reduce the quality of life for the affected patient population. Nearly 8.2 million individuals in the United States suffer from non-healing wounds each year (Nussbaum *et al*. 2020). Patients often experience debilitating symptoms such as severe pain, drastically reduced mobility, and emotional distress (Sen, 2020). This costs the United States alone over $50 billion annually to treat chronic non-healing wounds (Barbul *et al*. 2020).

The repair of cutaneous wounds is a complex process which is separated into four stages of wound healing: hemostasis, inflammation, proliferation, and tissue remodeling (Wilkinson *et al*. 2020). Hemostasis takes place immediately after an acute insult to blood vessels to reduce blood loss via clot formation. This is primarily accomplished with platelets, extracellular matrix (ECM) proteins and clotting factors (Elnar *et al*, 2009). This is followed by the inflammatory phase, which is characterized as the primary immune response to defend the body against pathogens and tissue damage. This is carried out at the time of injury by vasodilation of surrounding blood vessels and the recruitment of a host of immune cells to the wound site to activate and regulate the complex inflammatory pathway (Chen *et al*. 2017). The proliferation phase is responsible for closing the wound. Hours following the injury, there is an activation of endothelial cells, keratinocytes and fibroblasts that act to fill the wound and deposit ECM (Chen *et al*. 2007). Finally, remodeling spans the entirety of the healing process and ultimately involves primarily fibroblasts laying down a new ECM to replace the initial granulation tissue and restore proper structure and function to the tissue (Diegelmann and Evans 2004).

Chronic wounds occur when there is a disruption at any point in the healing process. For example, underlying metabolic conditions can cause a wound to remain in the inflammatory stage which leads to ulceration (Atkin 2019). Burns, however, can have unchecked inflammatory pathways which delay the transition into the proliferation stage and lead to hypertrophic scarring (Rowan *et al*. 2015). This disturbance of inflammation and delay in wound closure also drastically increases the likelihood of infection, necrosis, morbidity, and mortality (Church *et al*. 2006).

The clinical management of chronic wounds remains a major challenge. The vast majority of treatments currently available either target an underlying etiology, reduce the likelihood of tissue necrosis and infection, or create a moist environment that is conducive to healing. These techniques include surgical debridement, proper wound cleansing, antibiotics, and moisture retentive dressings, in addition to pain management (Shamsian 2021). As important as these treatments are, none of them address the core issues that are preventing the wound from going through the proper stages of healing. More advanced treatment options include skin grafts, negative-pressure wound therapy and hyperbaric oxygen (Sibbald *et al.* 2021). However, these are only available to carefully selected, low risk patients with smaller wounds and an established diagnosis. The rest of the population is left with therapies of limited efficacy supported by weak to mixed evidence at best (Sibbald *et al.* 2021). For this large subset of the patient population, as previously mentioned, chronic wounds often lead to chronic pain, severely reduced physical function, social isolation, and poorer mental health outcomes (Olsson *et al.* 2019)

In an attempt to address this issue, stem cells have become an exciting focus in the field of regenerative medicine. Stem cells have the ability to differentiate into different cell types, are self-renewing and have been shown to secrete specific proteins related to cell-to-cell signaling, all of which highlight their potential to be used to stimulate healing and accelerate wound closure (Kucharzewski *et al*. 2019). Many different stem cells exist, ranging from the totipotent embryonic morula, which can differentiate into all the cell types in the body, to the adult unipotent satellite cells which can only produce skeletal muscle cells (Kucia *et al*. 2007).

Mesenchymal stem cells (MSC) are commonly being used in therapies since they are generally more accessible to harvest while still being multipotent, meaning that they have the potential to differentiate into a variety of mesodermal lineages (Pittenger *et al*. 1999). Historically, the most common MSC used has been derived from bone marrow (BMSC) (Wu *et al.* 2007). In regards to wound healing, BMSCs have been extremely promising as they have shown a tremendous ability to expedite the closure of wounds on multiple occasions using either local injections, collagen matrices, or topical sprays (Kirby *et al.* 2015). However, there are some drawbacks to the harvesting and abundance of BMSCs. Not only is a bone marrow aspirate required, which can be quite painful and a source of morbidity, the amount of BMSCs in each aspirate is typically only about 0.001-0.01% of the entire sample (Mohamed-Ahmed *et al*. 2018).

Adipose-derived stem cells (ADSC) have recently been proposed as a substitute for BMSCs to avoid some of these problems (Mazini *et al*, 2020). Adipose tissue samples are typically obtained through minimally invasive procedures that cause little distress to patients. These are processed and through enzymatic isolation, the stromal vascular fraction (SVF) can be acquired (Nguyen *et al*. 2016). The SVF is the portion of adipose tissue which contains the ADSCs, and typically has a stem cell frequency of between 1-3% (Chatterjee *et al*. 2015). In addition to ADSCs being more abundant and easier to harvest, they have been shown to have very similar characteristics and potency to the BMSCs, and out preform BMSCs in regards to paracrine signaling and cell-to-cell communication (Minteer *et al*. 2013).

While these MSC trials are promising, there is ongoing controversy regarding their effectiveness and potential side effects (Bacakova *et al.* 2018). There is evidence to suggest that using MSCs therapeutically could potentially increase one's risk of various types of cancer due to the stem cells' proliferative potential (Mohr and Zwacka, 2018). Additionally, there is a considerable decline in stem cell potency, life-span and overall effectiveness with increased patient age (Nigro *et al*. 2018). Lastly, stem cell therapies must have either a matched allogeneic donor, which can be exceptionally difficult to find, or an autologous graft which forces the patient to have two separate operations. The need for two procedures is because the number of stem cells required is much greater than what can be acquired from harvested tissue in the first procedure, and therefore must be cultured *ex vivo* to expand their numbers before being administered therapeutically in a second procedure (Bura *et al*. 2014).

To avoid these issues, there has been a recent surge of research activities exploring the mechanism by which these stem cells act to improve wound healing in order to determine whether the physical stem cells need to be present at all. Already, studies have shown that MSCs are able to stimulate proliferation and migration to aid in wound closure (Li and Fu 2012). Moreover, purified MSC exosomes have been shown to be able to promote angiogenesis and re-epithelialization (Rani and Ritter 2016). Certain molecular signaling pathways, such as PI3K/Akt and Wnt/β-catenin which are active in MSCs, have also begun to be targeted as they may play a role in wound closure (Zhang *et al*. 2018; Mi *et al*. 2022).

Scratch assays are used as an *in vitro* model to study wound closure and can be used to examine different treatments to improve wound healing. This technique involves various types of epithelial cells being grown to confluency and this confluent plate is then scored with a pipette tip to simulate a wound (Mouritzen and Jenssen 2018). With these assays, various experiments have been conducted to test the efficacy MSCs have on wound closure, specifically examining MSC conditioned media and MSC exosomes (Mayo *et al*. 2017). One study found that using BMSC conditioned media increased the closure rate of both keratinocyte and fibroblast scratches and identified a couple of cytokines secreted in the conditioned media that may be involved with the increased closure rate (Walter *et al.* 2010).

However, there are several shortcomings associated with current stem cell research. First, most of these studies use immortalized cell lines of either keratinocytes or fibroblasts of human or rodent origin, which are easier to work with since they are typically genetically and/or phenotypically modified (Smits *et al*. 2017). In addition to this, because cell lines are modified at a cellular level, the results from this

research are not entirely reflective of primary human cells (Smits *et al*. 2017). Thirdly, as exciting as the experimentation is with conditioned media and purified exosomes collected from MSC only cultures, these studies lack any information on a co-culture wound closure environment of MSCs with keratinocytes or dermal fibroblasts. This type of co-culture could allow for communication in the simulated wound environment, which may alter the secretome. The concept that paracrine cross-talk between mammalian cells can alter their secretome has been shown before (Chatterjee *et al.* 2019).

This study conducted a scratch assay using primary human keratinocytes to test the effects of ADSCs on wound closure, using a transwell insert to allow the cells to communicate without direct cell contact, and to provide proof of principal that ADSCs and keratinocytes show a different secretome profile during wound closure co-cultures. SVF cells were used as source of primary human ADSCs, as opposed to bone marrow. Instead of immortalized cell lines, low passage primary human epithelial keratinocyte-adult (HEKa) cells were used to simulate cutaneous wounds. To achieve the project's objective, SVF cells were plated on a transwell insert with a porous membrane fine enough to prevent cell migration, but large enough to facilitate diffusion of cell secretions. These inserts were placed in wells containing HEKa cells at the bottom, which were scratched, to allow for paracrine signaling between the SVF cells and the HEKa cells during the entirety of the wound closure process.

The goals of the study were two-fold: a) demonstrate that ADSC-rich SVF could accelerate primary keratinocyte wound closure and, b) identify secreted cytokines present during this primary human keratinocyte wound closure caused by SVF-HEKa paracrine signaling.

## Materials and Methods

### *Keratinocyte Cell Cultures*

Primary human epidermal keratinocytes-adult (HEKa) cells were purchased from ThermoFisher Scientific (C0055C) used as the cell model system (Figure 1). HEKa cells were grown in cell culture plates containing Keratinocyte Growth Medium 2 (PromoCell) supplemented with bovine pituitary extract 0.004mL/mL, EGF 0.125ng/mL, insulin 5µg/mL, hydrocortisone 0.33µg/mL, epinephrine 0.39ug/mL, transferrin 10ug/mL, and $CaCl_2$ 0.06mM. No antibiotics or fungizones were added to the growth medium to ensure minimum alteration to these primary cells.

### *Stromal Vascular Fraction and Adipose-Derived Stem Cell Preparation*

Patients that undergo breast reconstruction operations following mastectomies often have fat grafts used as filler to improve contour and decrease scar tissue formation. Adipose tissue was harvested from leftover abdominal flaps used in such procedures. These fat grafts were collected based on informed patient consent as part of the Research Ethics Board approved protocol (HS24840 (H2021:165)). Samples were processed as previously described (Chatterjee *et al*. 2015). Briefly, the excess skin was removed from the abdominal flaps and the fat tissue was cut into 0.7-1.0 $cm^2$ pieces and subjected to enzymatic and mechanical dissociation overnight in a shaker flask containing Dulbecco's Modified Eagle Medium (DMEM), collagenase and hyaluronidase for 16-18h at 105-110rpm, 37ºC. The fibrotic tissue was removed, and samples washed with Hanks Balanced Salt Solution (HBS) containing 2% Fetal Bovine Serum (FBS). Samples were then resuspended in freezing medium containing a 50/50 mix of DMEM and FBS and 7% Dimethyl Sulfoxide (DMSO). The sample was cooled at – 80ºC for a minimum of 2.5h before being transferred to the vapor phase of a liquid nitrogen tank for long-term storage and future use.

On the day of experiments, frozen adipose tissue samples were thawed and further processed to isolate the SVF, as previously described (Chatterjee *et al*. 2015). Briefly, samples were thawed and

diluted in 10mL of Hanks containing 2% FBS before being centrifuged at 1200 rpm for 5min. The supernatant was removed to isolate the cell pellet, which was then resuspended in 1-2 mL of warm trypsin and gently mixed, before incubating for 5min in a 37ºC water bath. The sample was diluted with 2% Hank's, and the released cells were pelleted centrifugation as described. The supernatant was aspirated, and the pellet was resuspended in 1-2mL of dispase and 100-200 µL of DNase (1mg/mL) and incubated in a 37ºC water bath for 5min. After incubation, the sample was diluted in 10mL of cold 2% Hanks and then filtered through a 40µm cell strainer. This filtrate was then spun down at 1200 rpm for 5min, the supernatant was discarded, and the pellet was resuspended in 1mL of 2% Hanks. If the sample contained red blood cells, 4mL of cold ammonium chloride ($NH_4Cl$) was added before centrifuging again and resuspending in 1mL of 2% Hanks. The concentration of the sample was calculated by mixing 10µL of the sample with 10µL of trypan blue, plating on a hemocytometer and counting the number of cells per quadrant.

Immunomagnetic separation was then used to isolate CD31 and CD45 cells and remove them from the bulk population. CD31 and CD45 are cell surface markers found on epithelial cells and immune cells respectively. After CD31 and CD45 cells were removed, the remaining heterogeneous cell mixture was denoted as passage 0 SVF (P0SVF) and was ready for seeding.

***Stem Cell Potential Analysis***

Adipose derived stem cells are defined through the following: a) adherent to tissue culture plates, b) having the ability to differentiate into three different mesenchymal lineages, and c) ability to form fibroblast colonies (CFU-F) of 50 cells or more (Dominici *et al.* 2006). All primary SVF cells used in this project contained cells that were able to adhere to plastic tissue culture plates and were carried up to passage 3 in vitro (P3-SVF). In order to measure the sample's ability to form fibroblast colonies, 1000 P0-SVF or 200 P3-SVF cells were plated in each well of a 6-well plate containing MesenCult™ MSC Basal Medium (Human), supplemented with MesenCult™ MSC Stimulatory Supplement (Human) (StemCell Tech.) for 7-10 days. Cultures were then fixed in 1:1 mixture of acetone and methanol and individual fibroblast colonies were visualized using crystal violet dye. Colonies, defined as a grouping of over 50 cells, were counted using an inverted microscope (Figure 2a). The fibroblast colonies are used as proxy for ADSC numbers in each SVF sample (Figure 2b). Ratio paired, one tail t-tests were used to determine whether there was statistical significance between samples. Finally, the P0SVF cells were plated in a 24 well plate and grown separately for two weeks in growth conditions specifically designed to allow them to differentiate into osteogenic, adipogenic, and chondrogenic lineages (StemCell Tech). After two weeks, the cells were fixed in 4% formaldehyde and stained. The presence of bone matrix in these cultures was determined using Alizarian Red, the presence of mature adipocytes was determined using Oil Red O, and the presence of chondrocytes was determined using Alician Blue (Figure 3).

***Transwell Scratch Assay***

To set up the transwell scratch assay, a 24-well plate was plated with 50,000 keratinocytes (Figure 1) per well and allowed to grow out to be approximately 80-90% confluent over 4-5 days in an incubator, at 37ºC containing 5% $CO_2$. These HEKa wells would eventually be scratched as the simulated wounds.

P0SVF was plated at a density of 15,000 cells in transwell inserts with a porous membrane that allows for the passage of secreted factors but does not allow cells to pass through (Figure 1). These porous inserts allowed for paracrine communication between SVF and keratinocyte cells. SVF was plated in MesenCult™ MSC Basal Medium (Human), supplemented with MesenCult™ MSC Stimulatory Supplement (Human) (StemCell Tech.) for 24hrs in a similar incubator as described for the keratinocytes to allow for adherence. No antibiotics or fungizones were added to the growth medium to ensure minimum alteration to these primary cells.

After HEKa cells became confluent in the 24 well plate, the media was changed to serum free Keratinocyte Growth Medium 2 for 18-24hrs. This time period in serum starved media minimized cell proliferation and aligns all cell cycles in all plates to the G0 phase of the cell cycle, while causing minimal harm to the cells (Khammanit *et al*. 2008).

After the allotted time, the serum free media was removed, the HEKa wells were rinsed gently with phosphate buffered saline (PBS) and were then filled with fresh PBS. A scratch was introduced vertically down the middle of the well with a 1 mL pipette tip to create the simulated wound (Figure 1). This PBS was again gently mixed to remove any keratinocytes that may have been dislodged. Subsequently 600mL of Keratinocyte Growth Medium 2 with a custom-made supplement (EGF 0.125ng/mL; insulin 5ug/mL; hydrocortisone 0.33ug/mL; transferrin 10ug/mL; $CaCl_2$ 0.06mM) was added to the well. This slight alteration of the supplement was made to avoid excess proteins in the media so as to not dominate the secretome analysis that would follow. The SVF inserts were also washed with PBS and had their media changed to 100uL of Keratinocyte Growth Medium 2 with the same custom-made supplement previously described. The decision to switch all media to the custom keratinocyte media was made since any amount of Mesencult in co-culture had adverse effects on the keratinocytes, while the SVF cells were unaffected in the custom keratinocyte media for the duration of the scratch assay. The inserts containing the SVF cells were then placed into wells containing scratched keratinocytes at time zero (0h) to act as the experimental condition (Figure 1). Controls in these experiments included keratinocyte with scratches but without SVF inserts and SVF inserts in wells without keratinocytes. The 24 well plates containing the scratches were then placed in an incubator, at 37$^{o}$C containing 5% $CO_2$ for 36h. For the purposes of these experiments three different SVF samples were used (n=3), each with three technical replicates.

***Wound Closure Analysis***

Images of each scratch were taken with an EVOS M5000 microscope at the same location at 0h, 12h, 24, and 36h, or until there was complete scratch closure. These images were used to compare the rate of wound closure in the experimental co-culture of HEKa with SVF, against the HEKa alone control scratches. The scientific image analysis software ImageJ was utilized with a custom macro that was developed to measure the area of the scratch at each time point by identifying the scratch edge as well as any migrating cells in the scratch (Figure 4). The measurements of each test were standardized to the original scratch area and used to compare the percentage of wound closure in the HEKa alone controls against the HEKa with SVF co-cultures. Ratio paired, one tail t-tests were used to determine whether there was statistical significance between HEKa alone and HEKa with SVF samples at each time point.

***ELISA Secretome Analysis***

After 36hrs, the media from each well was transferred into Eppendorf tubes and frozen at –80$^{o}$C. These media were then sent to Eve Technology Corporation (Calgary) to analyze and compare the secreted cytokines from HEKa scratches alone (control), SVF cells alone (control) and co-culture of scratched HEKa scratches with SVF cells in transwell inserts (experimental arm). An enzyme-linked immunosorbent assay (ELISA) was used which quantified the concentration of 71 different human cytokines, chemokines and growth factors. To analyze the data, heat maps were generated to visualize the upregulation of cytokines found. The change in cytokine concentrations in the HEKa scratches with SVF cells in transwell inserts were normalized to HEKa scratches alone.

Statistical analysis was performed on targets of interest to determine whether the upregulation of cytokines found in HEKa scratches with SVF cells in transwell inserts was significant compared to HEKa scratches alone and SVF cells alone. Ratio paired, one tail t-tests were used to determine statistical significance.

### *P3 SVF Scratch Assay*

Aliquots of 15,000 cells from each P0SVF sample were grown out and replated until they reached passage 3 (P3-SVF) to examine their effects on keratinocyte wound closure. Once grown out to P3SVF, the same transwell scratch assay, image taking, and analysis was conducted as described above. In addition, CFU-F and trilineage differentiation experiments were also performed to demonstrate the stemness of P3 ADSCs.

## Results

### *Primary non-cultured and cultured human SVF cells contain adipose stem cells*

Three sets of experiments were conducted to determine the presence of ADSCs in SVF and to distinguish whether there were any differences between P0-SVF and P3-SVF samples. First, all P0-SVF and P3-SVF cells were successfully adhered to plastic tissue culture plates. Secondly, three specifically designed growth conditions were used to determine the differentiation potential of cells from each SVF sample to examine if they have the potential to differentiate into three mesenchymal cell lines. All P0-SVF and P3-SVF samples equally demonstrated the ability to differentiate into osteogenic, adipogenic and chondrogenic lineages (Figure 3). Finally, to determine the number of ADSCs in each SVF sample, single-cell suspensions prepared from the P0- and matching P3-SVF were placed in CFU-F assays and the fibroblast colonies were fixed, stained, and counted (Figure 2a). Approximately 2% of the P0-SVF cells were able to form fibroblast colonies of at least 50 cells, as compared to ADSC-enriched P3-SVF where nearly 25% of the cells were able to form fibroblast colonies (Figure 2b). This increase in ADSC concentration was found to be statistically significant ($p=0.03$*) and represents more than a 10x increase in ADSCs present in the P3-SVF compared to the initial P0-SVF.

### *ADSC-rich SVF shows accelerated keratinocyte wound closure*

In order to examine whether SVF cells accelerate wound closure, the rate of gap closure in transwell scratch assays set up with HEKa and SVF cells were observed and quantified over the course of 36 hours. In these experiments HEKa cells alone with a scratch and P0- or P3-SVF cells alone were used as controls. The scratched area of the plates (simulated wound area) was photographed and analyzed at 0h, 12h, 24h and 36h to determine if SVF containing inserts increased keratinocyte wound closure (Figure 5). Compared to the rate of wound closure in HEKa cell alone, HEKa with P0-SVF scratches showed a statistically significant increase in wound closure at 36h (Figure 6A, $p=0.04$*). Interestingly, P3-SVF cells not only improved wound closure at both the 24h ($p=0.005$*) and 36h ($p=0.008$*) timepoints compared to the HEKa alone scratches, but P3-SVF also showed enhanced closure compared to the matched P0-SVF sample (Figure 6B).

In both P0-SVF and P3-SVF conditions, primary human keratinocyte wound closure was accelerated compared to the HEKa alone condition. Moreover, the P3-SVF CFU-F (Figure 2b) and scratch assay results appear to show that an increased number of ADSCs may correlate with an increased acceleration of wound closure when compared to the matched P0-SVF sample and control data (Figure 6).

It is interesting to note that in these experiments, the SVF cells were plated in transwell inserts with a porous membrane that only allowed the passage of media and secretions (Figure 1). This design meant that there was never any cell-cell contact between HEKa cells and ADSCs, which indicates that the accelerated rate of wound closure by the P0-SVF and P3-SVF scratch assays was caused by secreted proteins. This is an essential finding which suggests that no direct cell-cell contact is required for SVF cells to improve wound closure.

***SVF Cells and Keratinocytes have an altered secretome during wound healing***

Since the transwell assays indicated that secreted proteins were responsible for the accelerated wound closure in HEKa scratches with SVF cells, we decided to examine which cytokines and growth factors were present during keratinocyte wound closure. For this purpose, growth media was collected from transwells containing either HEKa cells alone with scratch, P0-SVF alone, and P0-SVF and HEKa cells with scratch. The experiments were terminated when 80% wound closure was observed in the P0-SVF and HEKa cells transwells. One of the transwells with P0-SVF and HEKa cells reached 80% wound closure in 24 hours while the other 2 samples reached this endpoint in 36 hours. Growth media was also collected from the HEKa cells alone with a scratch and the P0-SVF cells alone to provide a set of controls. These growth media, that are also called conditioned media, were used in a multiplex ELISA assay (Eve Technologies, Calgary) to quantify the presence of cytokines and growth factors in each conditioned media. This is an immunological assay that detects and quantifies peptides, proteins, antibodies, and hormones in complex mixtures using specific antibodies.

This ELISA array consisted of 71 human cytokines, chemokines, and growth factors. For data analysis, priority was given to cytokines whose expression were significantly increased in P0-SVF/HEKa transwells during wound closure compared to the P0-SVF and HEKa cells alone. This analysis revealed 5 cytokines and 1 chemokine whose expression was negligible in the conditioned media obtained from HEKa and P0-SVF cells alone but showed statistically significant increase in the conditioned media obtained from the P0-SVF/HEKa cells transwells during wound closure (Table 1). Five targets were upregulated with statistical significance ($p \leq 0.05$) and one trending toward statistical significance when conducting ratio paired one tail t-tests were identified: IL-6 (p=0.01*), GRO-α (p=0.02*), IL-8 (p=0.03*), ENA-78 (p=0.04*), G-CSF (p=0.05*), and MCP-1 (p=0.08) (Figure 7).

These target cytokines were upregulated up to 175x during SVF-accelerated keratinocyte wound closure (Figure 7). The increase in levels of these 6 cytokines only seen in the HEKa scratches with P0SVF conditions indicates that the secretome from P0SVF and primary human keratinocytes is altered via paracrine signaling during wound healing. These observations are particularly interesting, since the HEKa alone cells with a scratch also show some level of wound closure and yet the level of these cytokines remains very low in these transwells.

As noted earlier, only two of the samples were taken to 36h and one was stopped at 24h due to premature complete wound closure. However, secretome profile of the P0-SVF/HEKa cell transwells show the same protein expression trends as the other two samples that showed wound closure in 36 hrs. As seen in Figure 7, G-CSF for example, appears to accumulate to a 27x increase in the 36h samples, while only having a 2x increase in the 24h sample.

The statistical analysis was based on the data obtained from all 3 biological samples from these experiments.

## Discussion

Throughout preliminary testing, the SVF cells showed an impressive ability to expedite wound closure of primary human keratinocyte. Importantly, these results align with current wound healing research with respect to stem cells obtained from the bone marrow being able to enhance cutaneous wound closure (Mohamed-Ahmed *et al*. 2018). However, the data provided in this project shows that SVF samples obtained from the patients' fat grafts could provide beneficial effects on healing of the severe burns and improving the clinical management of chronic non-healing cutaneous wounds.

By designing the experimental setup with primary human keratinocytes and SVF cells, the accelerated wound closure results are much more representative of the cells involved in wound healing in

living patients as opposed to the genetically modified immortal cell lines that are often used in similar studies (Smits *et al*. 2017). This is crucial to highlight because it offers more clinical relevance to the findings found here in our study.

Due to the heterogenic nature of SVF cells, it has been difficult to pinpoint exactly which cells or molecular signals are responsible for the accelerated wound closure observed in these scratch assays. However, by examining the HEKa scratches with P3-SVF compared to HEKa scratches with P0-SVF, we are starting to see indications that the ADSCs may in fact be the key factor in SVF's ability to accelerate wound closure. This hypothesis stems from the P3-SVF data showing significantly accelerated keratinocyte wound closure compared to the matched non-passage P0-SVF cells that contain 20x fewer adipose stem cells. (Figure 2b and Figure 6).

Most importantly, our results indicate that in a simulated wound environment, there is paracrine communication between SVF and primary human keratinocytes that alters their secretome. This paracrine crosstalk resulted in upregulation of 6 secreted factors during wound closure. Previous studies have shown that conditioned media from the bone marrow MSC's grown alone could improve wound closure and have even identified IL-6, IL-8, and MCP-1 as potential targets for wound healing (Walter *et al.* 2010). The data from our cytokine array also highlighted and identified these cytokines as being present in the SVF media alone, but at significantly lower concentrations than in the HEKa with SVF co-cultures during wound healing. Our data then indicates that the communication between the SVF cells and keratinocytes caused a significant upregulation in these cytokines, further highlighting the significant role paracrine signaling plays in wound closure. Additionally, our assay was able to identify ENA-78, G-GSF and GROα as novel targets for further study into their role in wound healing. It would be very interesting to examine if these six cytokines show significant upregulation in P3-SVF-accelarated keratinocyte wound closure.

Due to time restraints, the project was limited to the study of three patients' P0-SVF samples. Furthermore, one of these samples had the scratch assay halted and the media frozen at the 24h mark, as opposed to 36h. This decision was made since the wounds were already reaching full closure at 24h and there was concern that letting the plates become over-confluent over the next 12 hours may have detrimental effects on cell viability and subsequently on their secretome. The actual reason of this accelerated wound closure remains unclear however it is likely due to a smaller scratch area at the start of the experiment. Interestingly however, this discrepancy in wound closure time suggests that there may be a significant surge in cytokine secretion between 24-36h (Table 1). By the 24h timepoint, the same trends of upregulated cytokines of interest are seen, however they are closer to 1.5-2x fold increases, as opposed to the 20x-175x upregulations of same cytokines at 36h. Unfortunately, we only have one 24h time point and thus cannot draw any definitive conclusions in this regard.

Identification of the secreted factors responsible for the acceleration in wound closure is the next step towards a truly cell-free therapy for over 8 million patients suffering from chronic non-healing cutaneous wounds annually (Nussbaum *et al*. 2020). This type of cell-free, standardized therapy could theoretically be given to any patient with a chronic, non-healing wound without the requirement to find a matched donor, or obtaining autologous SVF samples, and it would eliminate the variability of current stem cell treatments and the risk of immune reaction and rejection. Additionally, a standardized preparation of these cytokines and growth factors could be utilized in emergency departments and trauma centers to decrease wound closure time to try to reduce the incidence of infections, tissue necrosis, and progression into chronic non-healing wounds.

Therefore, the immediate future of the project is to functionally test each of these cytokines of interest, in all possible permutations and combinations, in wound closure assays set up with HEKa cells and test their ability to increase the rate of wound closure. This type of testing will help narrow down which secreted factors are responsible for the observed expedited wound closure, to then move on to functional testing in more realistic skin equivalent models, in vivo animal wound healing models and

eventually clinical trials. So far IL-6, IL8, ENA-78, MCP-1, G-CSF and GROα are exciting possibilities that require more in-depth exploration.

Interleukin 6 (IL-6) is commonly involved in inflammation and immediate immune responses to wounds (Tanaka *et al.* 2014). IL-8 is also involved in immune responses by guiding neutrophils to the wound site to prevent potential infections (Brennan and Zheng 2007). ENA-78 (CXCL5) acts similarly to IL-8 as a potent chemoattractant and activator of neutrophils at wound sites (Walz *et al.* 1997). Although it is not mentioned much in MSC wound healing literature, ENA-78 is associated with IL-8 in other physiologic signaling pathways (Walz *et al.* 1997). This could indicate that combination of ENA-78 and IL-8 may be beneficial to wound healing. Monocyte chemoattractant protein-1 (MCP-1) is yet another chemokine that plays a role in the recruiting and activation of immune cells, including lymphocytes, neutrophils and monocytes (Deshmane, 2009). Granulocyte colony stimulating factor (G-CSF) has many characteristics that make it an interesting target in stem cell research. It is primarily a growth factor that stimulates the production of granulocytes, however it also stimulates bone marrow stem cells to produce more stem cells and it acts as an attractant for stem cells in the body (Mickiene *et al*. 2020). Finally, growth-regulated alpha protein (GROα), also known as CXCL1, is known for being a neutrophil chemoattractant which is released by keratinocytes (Frink *et al.* 2007).

While testing these selected cytokines, we also plan to subject these samples to an unbiased, mass-spec proteomics analysis to further identify proteins, cytokines and growth factors that could be responsible for the accelerated wound closure seen. It would be naïve to assume that the 71 cytokines that were tested are the only possibilities that could be responsible for the accelerated wound closure seen in the HEKa scratches with SVF cells on transwell inserts.

**Acknowledgements**

I would like to extend my gratitude to the University of Manitoba, Max Rady College of Medicine, and the Department of Immunology for their continued support and resources. Thank you specifically to Dr. Raouf, Stefan Balko and the rest of the lab members for their valuable insight and expertise. Finally, thank you to the department of surgery and section of plastic surgery for providing the adipose tissue samples required to make this project possible.

**Figures**

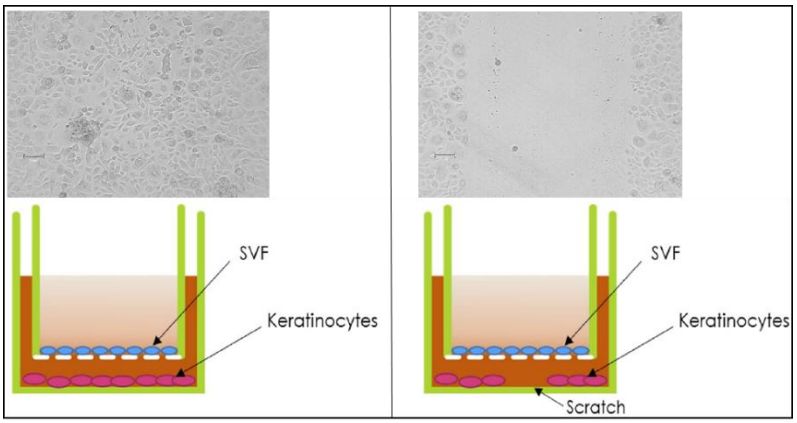


**Figure 1**. Transwell scratch assay. The stromal vascular fraction cells were obtained from patients' fat grafts and plated in transwells with a porous membrane and inserted into each well of 24-well tissue culture plates with primary human keratinocyte (HEKa) cells with scratches. Scratches were made with a 1mL pipette tip to simulate a wound area.

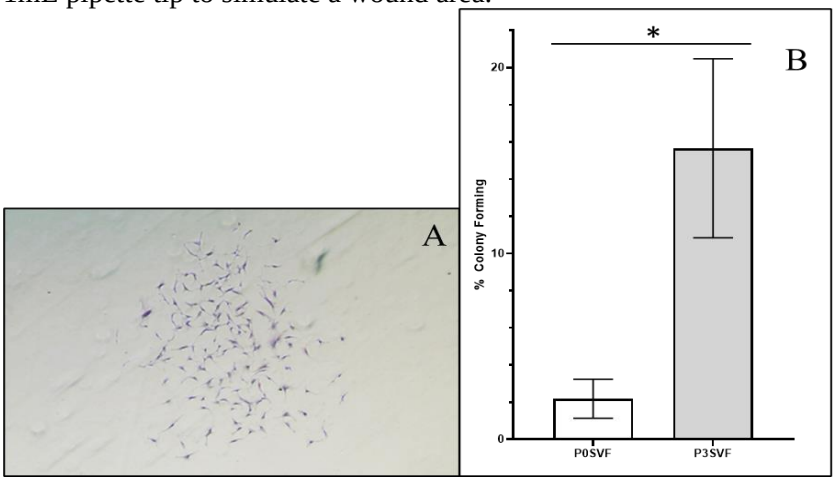


**Figure 2**. Minimally passaged SVF cells contain a significant number of stem cells
A) non-passaged SVF cells were placed in colony forming unit-fibroblast (CFU-F) assays. A representative fibroblast colony after 10 days is shown in the picture (10x magnification). B) Cells from P0-SVF and matching P3-SVF cells were placed in CFU-F assays and the fibroblast colony counts were used as proxies for ADSC numbers in each SVF sample. Mean and standard deviation from 3 SVF samples are shown in a bar graph (p=0.03*).

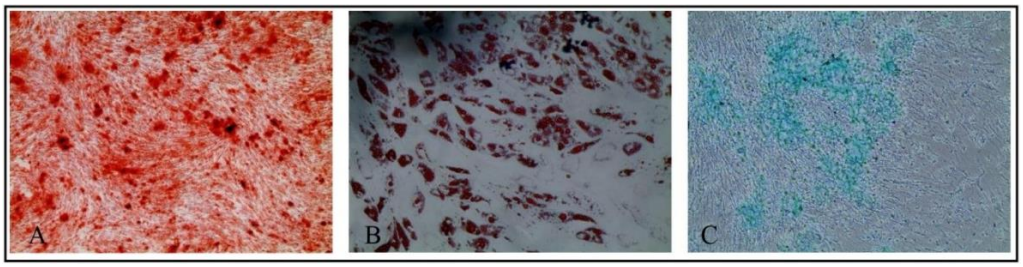


**Figure 3**. Adipose-derived stem cells are capable of trilineage differentiation. P0-SVF and P3-SVF cells were placed in specialized culture conditions and the presence of (A) bone matrix (xx, red color), (B) adipocytes (yy, dark red stains), and (C) chondrocytes (zz, blue color stain) were determined. Representative pictures from each culture are shown here. Pictures were taken at 10x magnification.

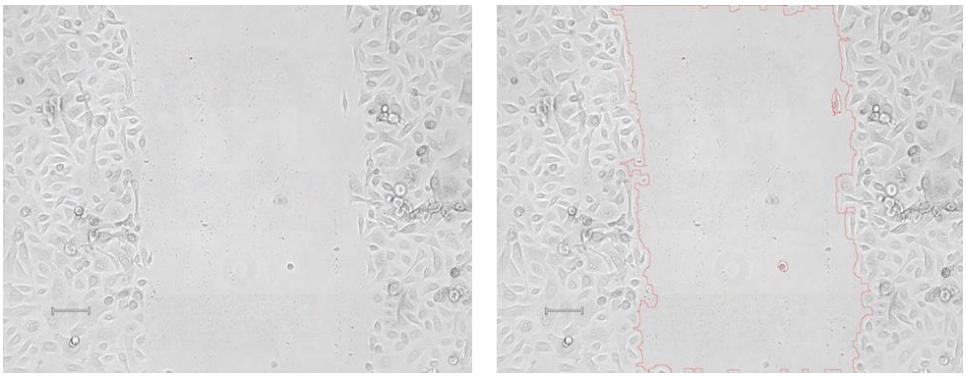

**Figure 4**. Wound closure analysis. Digital pictures were taken at 10x magnification from the transwell scratch assays on various hours and the image analysis software, ImageJ with a custom developed macro was used to quantify the scratch area in each image. The software identified the wound edge (red lines) and the area of the scratch at each timepoint was determined based on pixel intensity.

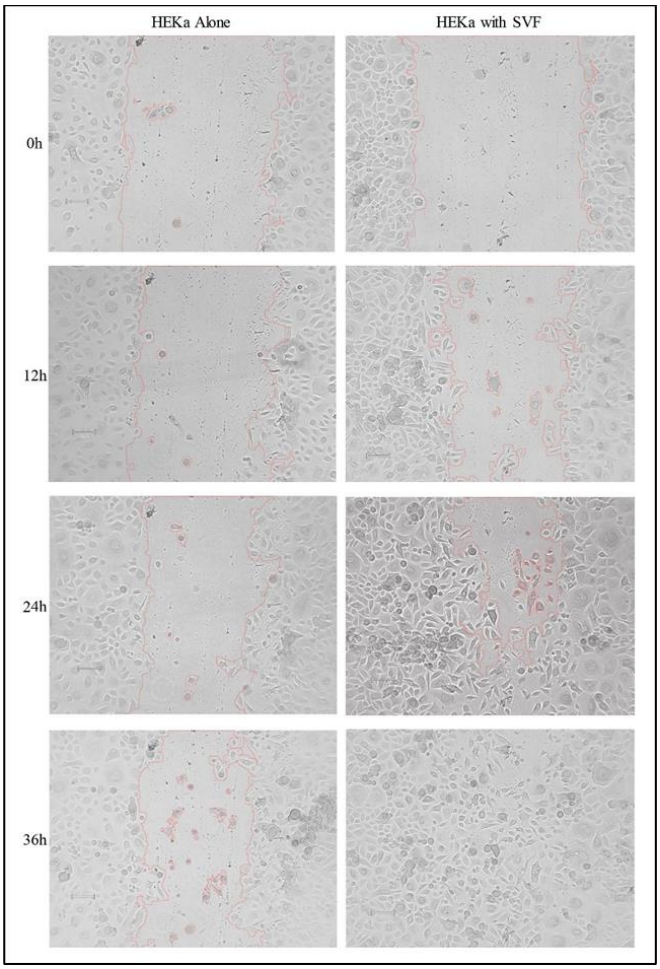


**Figure 5**. Sequential wound closure can be documented over 36h. Representative images showing increased wound closure over 36h in the HEKa scratch assays with P0-SVF co-culture, scratch assays with HEKa alone are depicted in the pictures (10x magnification).

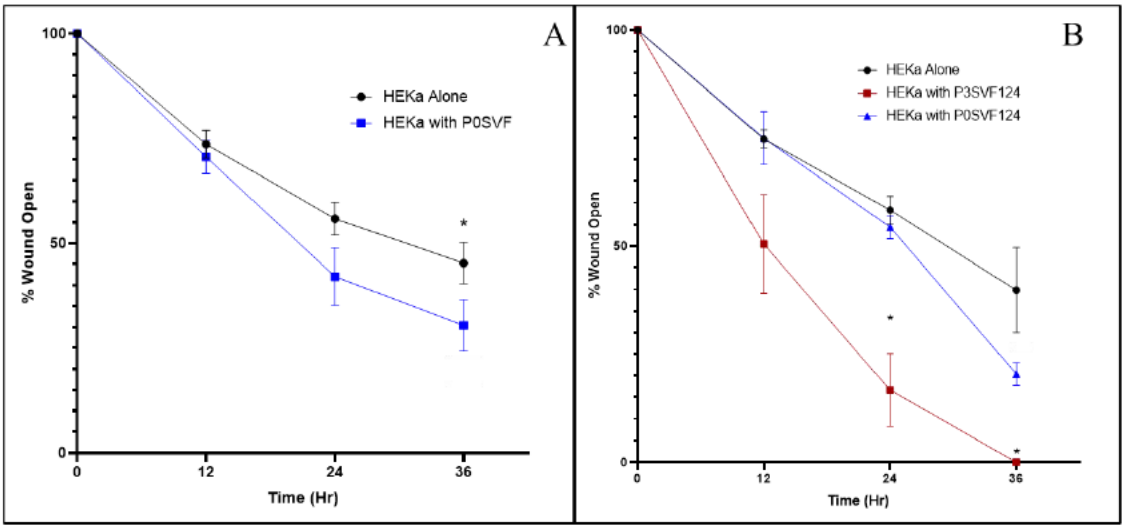


**Figure 6**. SVF cells accelerate keratinocyte wound closure. Transwell scratch assays were set up with HEKa cells alone or with P0-SVF (A) or P3-SVF (B) cells and wound closure rates were quantified and shown as percent wound (scratch) remaining open. HEKA with P0-SVF showed significantly more wound closure than HEKa alone in 36h (p=0.04*). Mean and standard error from 3 SVF samples are shown. B) HEKa with P3-SVF showed significantly more wound closure than HEKa alone at 24h (p=0.005*) and 36h (p=0.008*) and the HEKa cells with and the matching P0-SVF at 36h (p=0.008*). Mean and standard error from 1 P0- and matching P3-SVF sample with 3 technical replicates is shown.

| | 36h | | | | | 24h | | |
|---|---|---|---|---|---|---|---|---|
| | P0SVF124 | | P0SVF123 | | | P0SVF104 | | |
| | **HEKa Alone** | **HEKa+ SVF** | **HEKa Alone** | **HEKa+ SVF** | **SVF Alone** | **HEKa Alone** | **HEKa+ SVF** | **SVF Alone** |
| **GROα** | **373.92** | **540.30** | **601.85** | **730.57** | **0.00** | **131.97** | **175.52** | **0.00** |
| **IL-6** | **0.84** | **296.89** | **0.80** | **117.71** | **0.62** | **0.26** | **7.08** | **0.31** |
| **MCP-1** | **6.29** | **172.79** | **6.61** | **210.83** | **13.96** | **5.34** | **6.29** | **0.19** |
| **IL-8** | **175.25** | **974.03** | **150.44** | **763.23** | **2.19** | **73.11** | **151.62** | **0.51** |
| **G-CSF** | **9.69** | **282.94** | **9.69** | **240.37** | **0.00** | **6.56** | **13.72** | **0.00** |
| **ENA-78** | **33.18** | **547.36** | **82.92** | **463.85** | **0.00** | **7.72** | **21.33** | **0.00** |
| **IL-18** | 3.55 | 3.17 | 2.58 | 3.43 | OOR < | 4.90 | 6.85 | OOR < |
| **IL-1β** | 1.60 | 2.18 | 1.25 | 1.72 | 0.09 | 2.88 | 3.80 | 0.44 |
| **IFN-α2** | 20.71 | 15.81 | 5.95 | 12.48 | OOR < | 18.99 | 24.87 | OOR < |
| **IL-22** | 31.96 | 26.27 | 19.78 | 22.99 | OOR < | 27.79 | 21.44 | OOR < |
| **BCA-1** | 0.28 | 0.28 | 0.28 | 0.20 | 0.36 | 0.31 | 0.36 | 0.15 |

**Table 1**. Cytokine array analysis of HEKa and P0-SVF conditioned media. Cytokine levels obtained from an ELISA assay were reported as concentrations (pg/mL) based on standard curves. A subset of the 71-plex array is shown here with the cytokines of interest highlighted in bold colors based on their higher expression in HEKa with P0-SVF transwell scratch assays compared to HEKa or SVF alone cells.

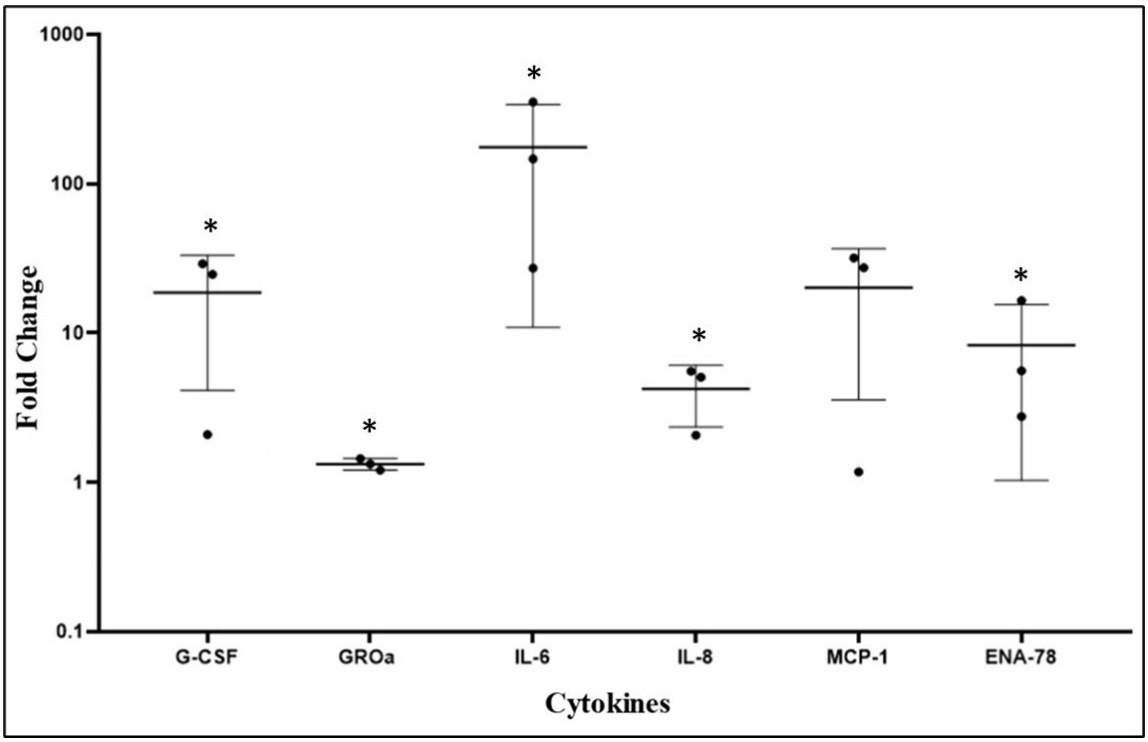


**Figure 7**. P0-SVF and HEKa cells show a different cytokine profile in transwell scratch assay. Increased cytokine concentrations from figure 6 were calculated based on cytokine levels in HEKa transwell scratch assays and shown in a graph. Based on ratio paired, one tail t-tests; IL-6* (p=0.012), GRO-α* (p=0.015), IL-8* (p=0.0249), ENA-78* (p=0.0354), G-CS*F (p=0.052), and MCP-1 (p=0.082) levels were found to be increased. This was pooled data from three different P0-SVF samples.

**References**


1. Chatterjee S, Bhat V, Berdnikov A, et al. Paracrine Crosstalk between Fibroblasts and ER+ Breast Cancer Cells Creates an IL1β-Enriched Niche that Promotes Tumor Growth. *iScience*. 2019;19:388-401. doi:10.1016/j.isci.2019.07.034
2. Chatterjee S, Laliberte M, Blelloch S, et al. Adipose-derived stromal vascular fraction differentially expands breast progenitors in tissue adjacent to tumors compared to healthy breast tissue. *Plast Reconstr Surg*. 2015;136(4):e414-e425. doi:10.1097/PRS.0000000000001635
3. Frink M, Hsieh YC, Hsieh CH, et al. Keratinocyte-derived chemokine plays a critical role in the induction of systemic inflammation and tissue damage after trauma-hemorrhage. *Shock*. 2007;28(5):576-581. doi:10.1097/shk.0b013e31814b8e0d
4. Deshmane SL, Kremlev S, Amini S, Sawaya BE. Monocyte chemoattractant protein-1 (MCP-1): An overview. *J Interf Cytokine Res*. 2009;29(6):313-325. doi:10.1089/jir.2008.0027
5. Mouritzen MV, Jenssen H. Optimized Scratch Assay for In Vitro Testing of Cell Migration with an Automated Optical Camera. *J Vis Exp*. 2018;(August):1-6. doi:10.3791/57691
6. Rani S, Ritter T. The Exosome - A Naturally Secreted Nanoparticle and its Application to Wound Healing. *Adv Mater*. Published online 2016:5542-5552. doi:10.1002/adma.201504009
7. Smits JPH, Niehues H, Rikken G, et al. Immortalized N / TERT keratinocytes as an alternative cell source in 3D human epidermal models. *Sci Rep*. 2017;(May):1-14. doi:10.1038/s41598-017-12041-y
8. Mi Y, Zhong L, Lu S, et al. Quercetin promotes cutaneous wound healing in mice through Wnt / β -catenin signaling pathway. *J Ethnopharmacol*. 2022;290(January). doi:10.1016/j.jep.2022.115066
9. Sen CK. Human Wound and Its Burden : Updated 2020 Compendium of Estimates. *Wound Heal Soc*. 2021;10(5):281-292. doi:10.1089/wound.2021.0026
10. Khammanit R, Chantakru S, Kitiyanant Y, Saikhun J. Effect of serum starvation and chemical inhibitors on cell cycle synchronization of canine dermal fibroblasts. *Theriogenology*. 2008;70(1):27-34. doi:10.1016/j.theriogenology.2008.02.015
11. Nussbaum SR, Carter MJ, Fife CE, et al. An Economic Evaluation of the Impact , Cost , and Medicare Policy Implications of Chronic Nonhealing Wounds. *Value Heal*. 2018;21(1):27-32. doi:10.1016/j.jval.2017.07.007
12. Elnar T V, Ailey TB. The Wound Healing Process : an Overview of the Cellular and Molecular Mechanisms. *J Int Med Res*. 2009;37(5):1528-1542.
13. Chen L, Dipietro LA. Toll-Like Receptor Function in Acute Wounds. *Wound Heal Soc*. 2017;6(10):344-355. doi:10.1089/wound.2017.0734
14. Church D, Elsayed S, Reid O, Winston B, Lindsay R. Burn Wound Infections. *Clin Microbiol Rev*. 2006;19(2):403-434. doi:10.1128/CMR.19.2.403
15. Rowan MP, Cancio LC, Elster EA, et al. Burn wound healing and treatment : review and advancements. *Crit Care*. Published online 2015:1-12. doi:10.1186/s13054-015-0961-2
16. Kucharzewski M, Rojczyk E, Wilemska-kucharzewska K, Wilk R, Hudecki J, Los MJ. Novel trends in application of stem cells in skin wound healing. *Eur J Pharmacol*. 2019;843(November 2018):307-315. doi:10.1016/j.ejphar.2018.12.012
17. Walz A, Schmutz P, Mueller C, Schnyder-Candrian S. Regulation and function of the CXC chemokine ENA-78 in monocytes and its role in disease. *J Leukoc Biol*. 1997;62(5):604-611. doi:10.1002/jlb.62.5.604
18. Olsson M, Järbrink K, Divakar U, Bajpai R. The humanistic and economic burden of chronic wounds : A systematic review. *Wound Repair Regen*. Published online 2019:5-7. doi:10.1111/wrr.12683
19. Bacakova L, Zarubova J, Travnickova M, et al. Stem cells : their source , potency and use in regenerative therapies with focus on adipose-derived stem cells – a review. *Biotechnol Adv*. 2018;36(4):1111-1126. doi:10.1016/j.biotechadv.2018.03.011

20. Mickiene G, Dalgėdienė I, Zvirblis G, et al. Human granulocyte-colony stimulating factor (G-CSF)/stem cell factor (SCF) fusion proteins: Design, characterization and activity. *PeerJ*. 2020;8:1-23. doi:10.7717/peerj.9788
21. Tanaka T, Narazaki M, Kishimoto T. IL-6 in Inflammation, Immunity, and Disease. *Cold Spring Harb Perspect Biol*. 2014;6(Kishimoto 1989):1-16.
22. Bishara N. The Use of Biomarkers for Detection of Early- and Late-Onset Neonatal Sepsis. *Hematol Immunol Infect Dis Neonatol Quest Controv*. 2012;2:303-315. doi:10.1016/b978-1-4377-2662-6.00018-3
23. Pittenger MF, Mackay AM, Beck SC, et al. Multilineage Potential of Adult Human Mesenchymal Stem Cells. *Sci Mag*. 1999;284(April):143-148.
24. Kucia M, Wu W, Ratajczak MZ. Bone Marrow-Derived Very Small Embryonic- Like Stem Cells : Their Developmental Origin and Biological Significance. *Dev Dyn*. 2007;(May):3309-3320. doi:10.1002/dvdy.21180
25. Wu Y, Wang J, Scott PG, Tredget EE. Bone marrow-derived stem cells in wound healing : a review. *Wound Repair Regen*. Published online 2007. doi:10.1111/j.1524-475X.2007.00221.x
26. Mohamed-ahmed S, Fristad I, Lie SA, et al. Adipose-derived and bone marrow mesenchymal stem cells : a donor-matched comparison. *Stem Cell Res Ther*. Published online 2018:1-15.
27. Minteer D, Marra KG, Rubin JP. Adipose-Derived Mesenchymal Stem Cells : Biology and Potential Applications. *Adv Biochem Eng Biotechnol*. 2013;(July 2012):59-71. doi:10.1007/10
28. Mohr A, Zwacka R. The future of mesenchymal stem cell-based therapeutic approaches for cancer e From cells to ghosts. *Cancer Lett*. 2018;414:239-249. doi:10.1016/j.canlet.2017.11.025
29. Nguyen A, Guo J, Banyard DA, et al. Stromal vascular fraction : A regenerative reality ? Part 1 : Current concepts and review of the literature. *Br J Plast Surg*. 2016;69(2):170-179. doi:10.1016/j.bjps.2015.10.015
30. Bura A, Planat-benard V, Bourin P, et al. Phase I trial : the use of autologous cultured adipose-derived stroma / stem cells to treat patients with non-revascularizable critical limb ischemia. *J Cytotherapy*. 2014;16(2):245-257. doi:10.1016/j.jcyt.2013.11.011
31. Mayo T De, Conget P, Becerra-bayona S, Sossa CL, Galvis V, Arango-rodrı ML. The role of bone marrow mesenchymal stromal cell derivatives in skin wound healing in diabetic mice. *PLoS One*. Published online 2017:1-17.
32. Nigro P, Bassetti B, Cavallotti L, Catto V, Carbucicchio C, Pompilio G. Cell therapy for heart disease after 15 years : Unmet expectations. *Pharmacol Res*. 2018;127:77-91. doi:10.1016/j.phrs.2017.02.015
33. Kirby GTS, Mills SJ, Cowin AJ, Smith LE. Stem Cells for Cutaneous Wound Healing. *Biomed Res Int*. 2015;2015.
34. Diegelmann RF. Wound Healing : An Overview of Acute , Fibrotic and Delayed Healing. *Front Biosci*. 2004;(June). doi:10.2741/1184
35. Wilkinson HN, Hardman MJ, Wilkinson HN. Wound healing : cellular mechanisms and pathological outcomes. *Open Biol*. Published online 2020.
36. Sibbald RG, Hons D, Derm FM, Health P. Wound Bed Preparation 2021. *Adv Skin Wound Care*. 2023;0(April 2021):183-195. doi:10.1097/01.ASW.0000733724.87630.d6
37. Li H, Fu X. Mechanisms of action of mesenchymal stem cells in cutaneous wound repair and regeneration. *Cell Tissue Res*. Published online 2012:371-377. doi:10.1007/s00441-012-1393-9
38. Li J, Chen J, Kirsner R. Pathophysiology of acute wound healing. *Clin Dermatol*. Published online 2007:9-18. doi:10.1016/j.clindermatol.2006.09.007
39. Zhang W, Bai X, Zhao B, et al. Cell-free therapy based on adipose tissue stem cell-derived exosomes promotes wound healing via the PI3K / Akt signaling pathway. *Exp Cell Res*. 2018;370(2):333-342. doi:10.1016/j.yexcr.2018.06.035

40. Walter MNM, Wright KT, Fuller HR, Macneil S, Johnson WEB. Mesenchymal stem cell-conditioned medium accelerates skin wound healing : An in vitro study of fibroblast and keratinocyte scratch assays. *Exp Cell Res*. 2010;316(7):1271-1281. doi:10.1016/j.yexcr.2010.02.026
41. Mazini L, Rochette L, Admou B, Amal S, Malka G. Hopes and Limits of Adipose-Derived Stem Cells ( ADSCs ) and Mesenchymal Stem Cells ( MSCs ) in Wound Healing. *Int J Mol Sci*. Published online 2020.
42. Dominici M, Le Blanc K, Mueller I, et al. Minimal criteria for defining multipotent mesenchymal stromal cells. The International Society for Cellular Therapy position statement. *Cytotherapy*. 2006;8(4):315-317. doi:10.1080/14653240600855905
43. Barbul A, Gelly H, Masturzo A. The Health Economic Impact of Living Cell Tissue Products in the Treatment of Chronic Wounds : A Retrospective Analysis of Medicare Claims Data. *Adv Skin Wound Care*. 2020;(January):27-34. doi:10.1097/01.ASW.0000581588.08281.c1
44. Shamsian N. Wound bed preparation: an overview. *Br J Community Nurs*. 2021;(September).
45. Powers JG, Higham C, Broussard K, Phillips TJ. Chronic wound care and management. *J Am Dermatology*. 2019;74(4):607-625. doi:10.1016/j.jaad.2015.08.070
46. Atkin L. Chronic wounds: the challenges of appropriate management. *Br J Community Nurs*. 2019;(September).